

Supporting Information

Poresize-controlled Gases and Alcohols Separation within Ultramicroporous Homochiral Lanthanide-Organic Frameworks

Zhongjun Lin,^a Ruqiang Zou,^{a,*} Jie Liang,^b Wei Xia,^a Dingguo Xia,^a Yingxia Wang,^b Jianhua Lin,^b Tongliang Hu,^d Qiang Chen,^d Xidong Wang,^a Yusheng Zhao,^a and Anthony K. Burrell^{c,*}

^a College of Engineering, Peking University, Beijing 100871, China. E-mail: rzou@pku.edu.cn. ^b College of Chemistry and Molecule Engineering, Peking University, Beijing 100871, China. ^c Chemical Sciences and Engineering Division, Argonne National Laboratory, 9700 S. Cass Avenue, Argonne, IL 60439. E-mail: Burrell@anl.gov. ^d Department of Chemistry, Nankai University, Beijing 300071, China.

Table S1 Selected bond distances (Å) and angles (°) for **1**.

Ce(1)-O(3)#1	2.403(8)	Ce(1)-O(2)#5	2.509(7)
Ce(1)-O(3)#2	2.403(8)	Ce(1)-O(1W)	2.539(15)
Ce(1)-O(1)#3	2.497(8)	Ce(1)-O(1)	2.497(8)
Ce(1)-O(2)#4	2.509(7)		
O(1)#3-Ce(1)-O(1)	150.2(5)	O(3)#1-Ce(1)-O(2)#4	137.9(3)
O(3)#1-Ce(1)-O(3)#2	77.3(5)	O(3)#2-Ce(1)-O(2)#4	72.5(3)
O(3)#1-Ce(1)-O(1)#3	126.2(3)	O(1)#3-Ce(1)-O(2)#4	75.8(3)
O(3)#2-Ce(1)-O(1)#3	79.1(4)	O(1)-Ce(1)-O(2)#4	95.8(3)
O(3)#1-Ce(1)-O(1)	79.1(4)	O(3)#1-Ce(1)-O(2)#5	72.5(3)
O(3)#2-Ce(1)-O(1)	126.2(3)	O(3)#2-Ce(1)-O(2)#5	137.9(3)
O(1)#3-Ce(1)-O(2)	142.3(3)	O(1)#3-Ce(1)-O(2)#5	95.8(3)
O(1)-Ce(1)-O(2)	49.3(2)	O(1)-Ce(1)-O(2)#5	75.8(3)
O(2)#4-Ce(1)-O(2)	68.8(3)	O(2)#4-Ce(1)-O(2)#5	147.1(3)
O(2)#5-Ce(1)-O(2)	121.0(2)	O(3)#1-Ce(1)-O(1W)	141.4(2)
O(1W)-Ce(1)-O(2)	105.79(16)	O(1)#3-Ce(1)-O(1W)	75.1(2)
O(3)#1-Ce(1)-O(2)#3	78.5(3)	O(1)-Ce(1)-O(1W)	75.1(2)
O(3)#2-Ce(1)-O(2)#3	77.0(3)	O(2)#4-Ce(1)-O(1W)	73.56(16)
O(1)#3-Ce(1)-O(2)#3	49.3(2)	O(2)#5-Ce(1)-O(1W)	73.56(16)
O(1)-Ce(1)-O(2)#3	142.3(3)	O(3)#1-Ce(1)-O(2)	77.0(3)
O(2)#4-Ce(1)-O(2)#3	121.0(2)	O(3)#2-Ce(1)-O(2)	78.5(3)
O(2)#5-Ce(1)-O(2)#3	68.8(3)	O(2)-Ce(1)-O(2)#3	148.4(3)
O(1W)-Ce(1)-O(2)#3	105.79(16)		

^a Symmetry transformations used to generate equivalent atoms: #1 x-y,-y+1,-z+2; #2 x,y+1,z;

#3 x-y+1,-y+2,-z+2; #4 -y+2,-x+2,-z+11/6; #5 x-y+1,x,z+1/6; #6 -y+1,-x+1,-z+11/6; #7

y,-x+y+1,z-1/6; #8 x,y-1,z

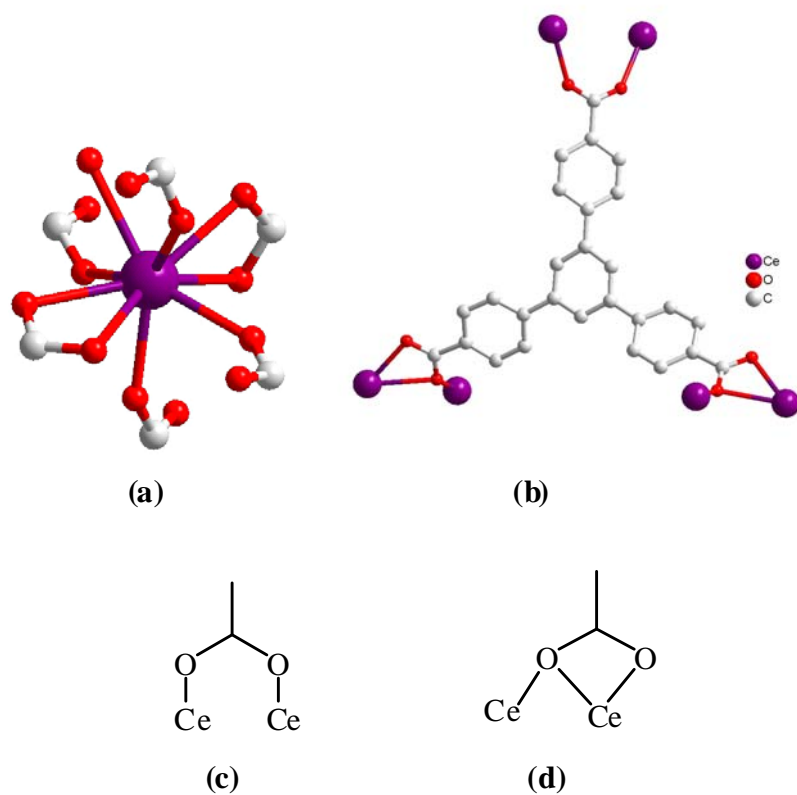


Figure S1. (a) The coordination environment of Ce(III). (b) The coordination environment of BTB ligand. (c) and (d) The two types of binding modes of BTB ligand.

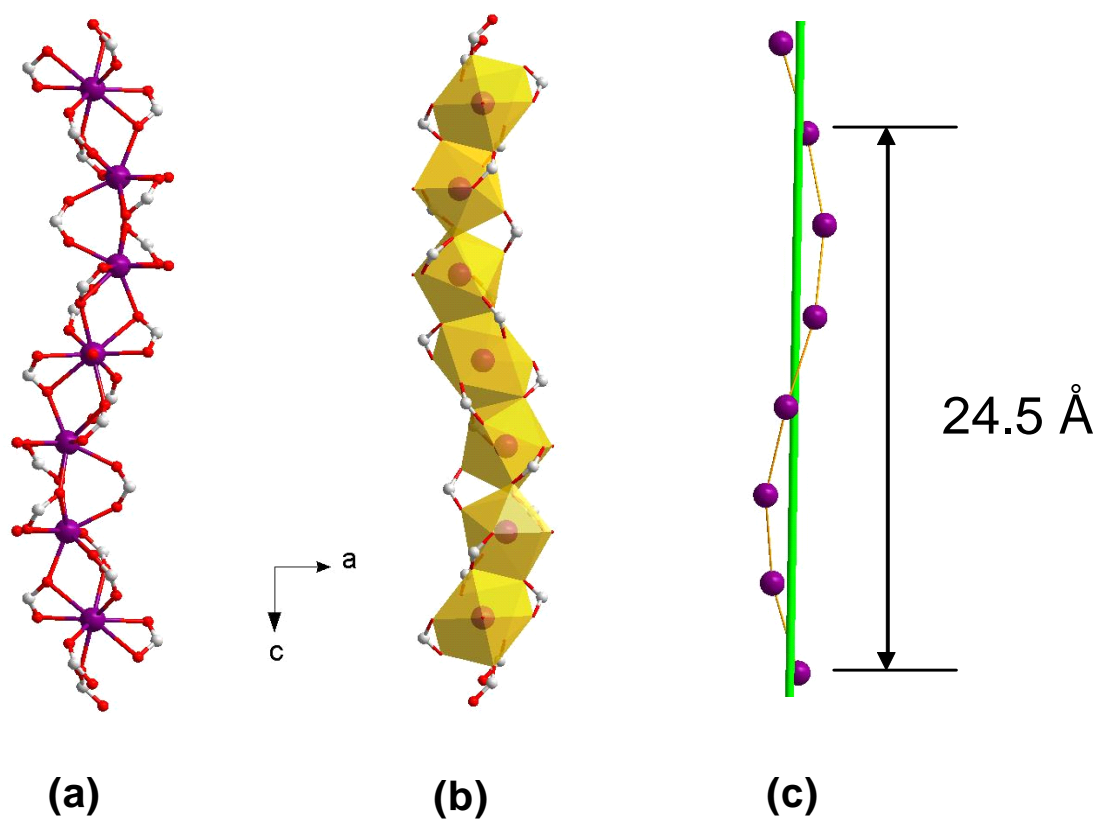


Figure S2. (a) and (b) One-dimensional inorganic chain along *c* direction. (c) Helical right-hand metal chain showing seven Ce (III) ions in a unit.

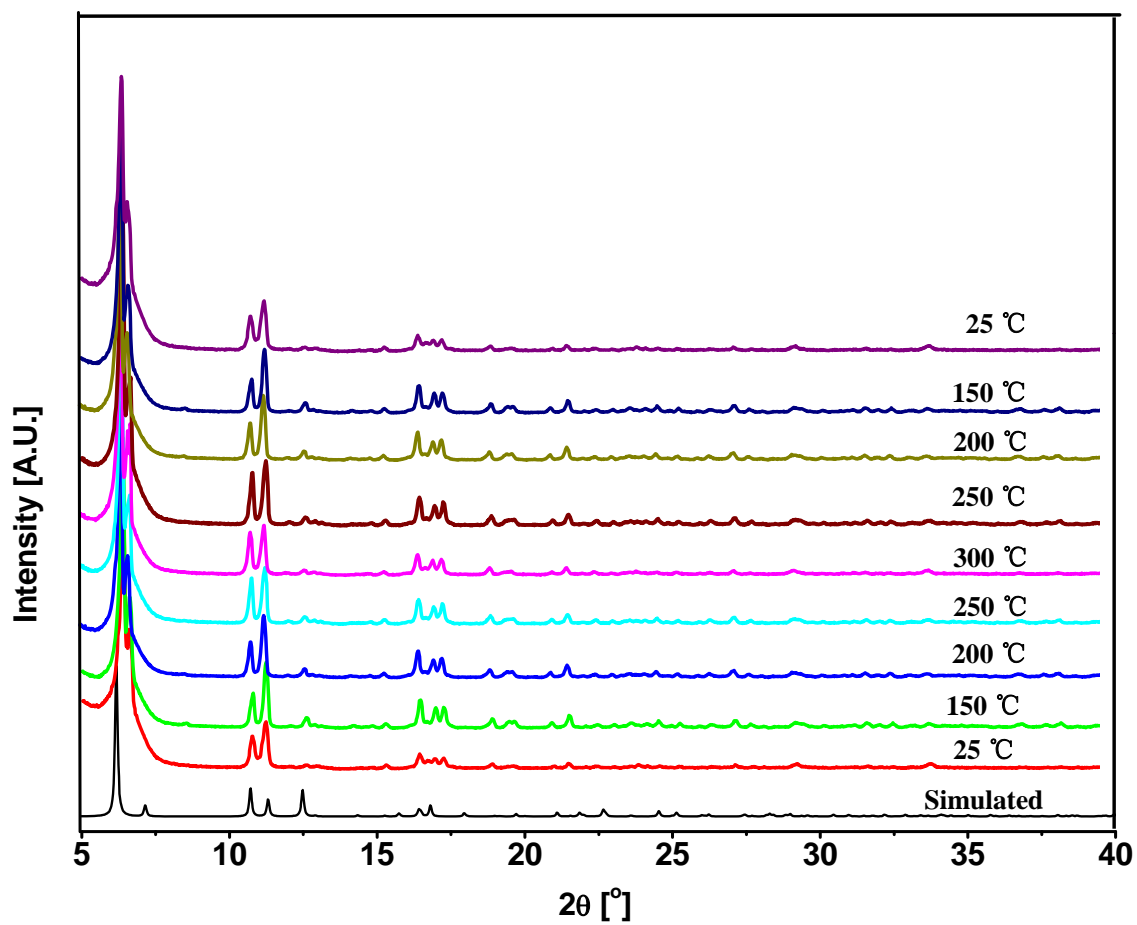


Figure S3. Temperature-dependent PXRD patterns of **1** in vacuum.

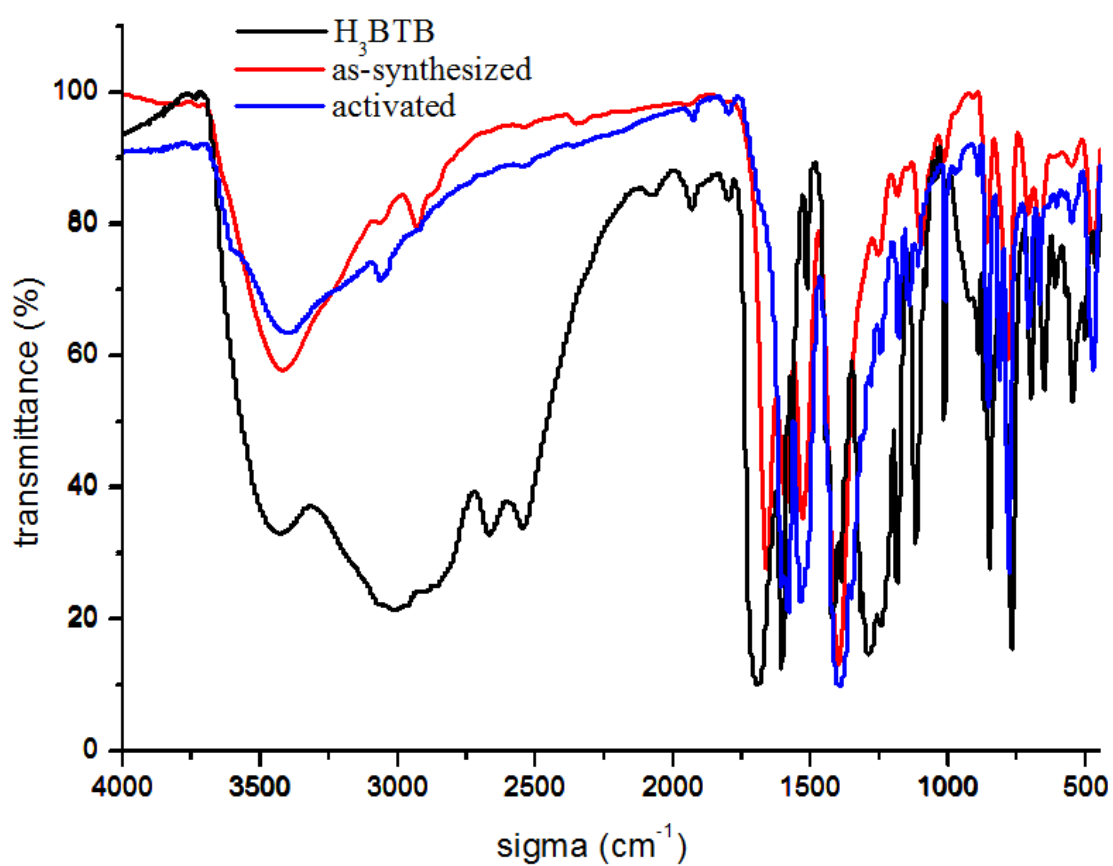


Figure S4. FTIR spectra of H₃BTB ligand, as-synthesized sample and activated sample.

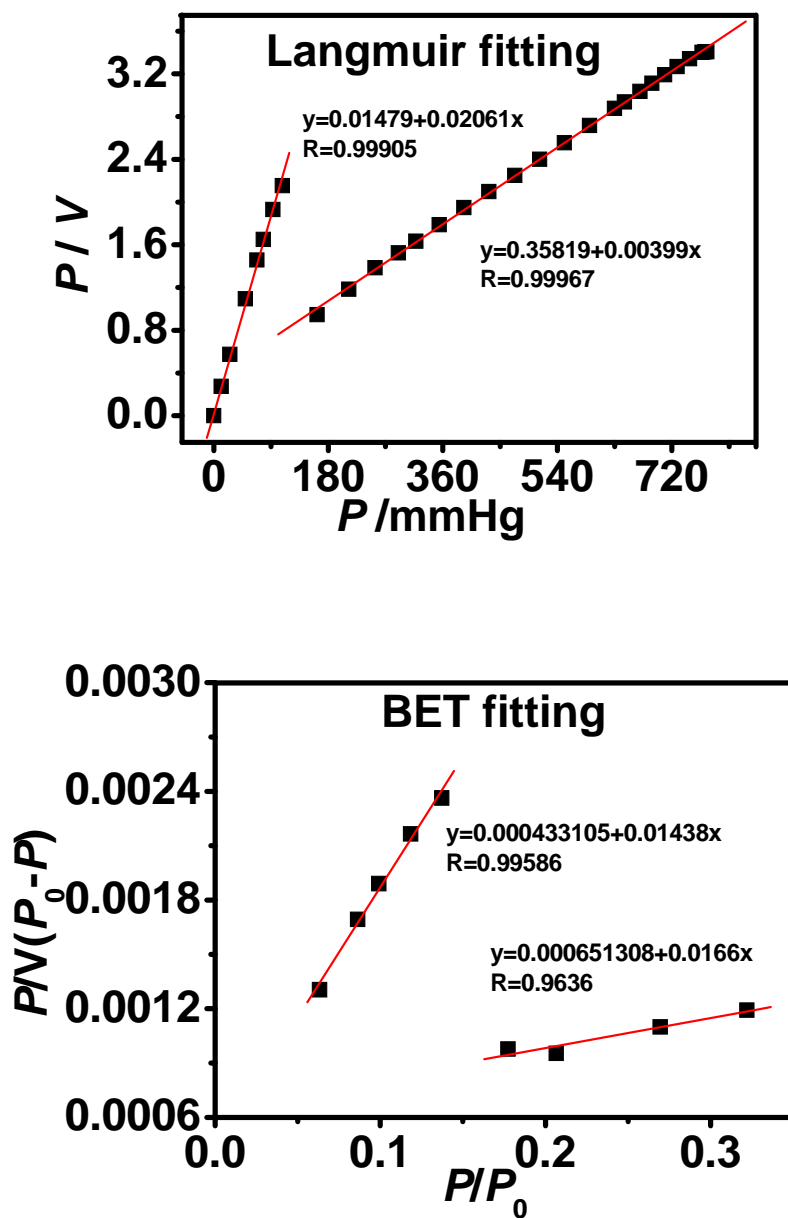


Figure S5. Langmuir fitting and BET fitting for N_2 adsorption isotherm at 77K.

The selectivity for CO₂/N₂, CH₄/N₂ and CO₂/CH₄ were calculated from the Henry constants.⁽¹⁾ The CO₂ adsorption isotherm was analysed by using a model based on dual-site Langmuir isotherm model [Eq (1)].

$$V(\text{CO}_2) = \frac{V_1 K_1 P}{1 + K_1 P} + \frac{V_2 K_2 P}{1 + K_2 P} \quad (1)$$

$V(\text{CO}_2)$ is the total volume adsorbed of CO₂; V_1 and V_2 , calculated adsorbed volume of CO₂ for the two contributions of the dual site Langmuir Isotherm; K_1 and K_2 , calculated stability constants of CO₂ adsorption for the two contributions of the dual site Langmuir isotherm. P is the applied pressure.

The experimental data corresponding to the CH₄ and N₂ adsorption isotherms were analysed by using single Langmuir isotherms [Eq (2)].

$$V = \frac{V_1 K_1 P}{1 + K_1 P} \quad (2)$$

V_1 , calculated adsorbed volume of CH₄; K_1 , calculated affinity constants;

Fitting of the adsorption branch for CO₂, CH₄ and N₂ based on the Langmuir isotherm models allowed us to calculate the Henry constants. For CO₂, $H(\text{CO}_2) = K_1 \times V_1 + K_2 \times V_2$, and for other gases, $H = K_1 \times V_1$.

The Henry law selectivity for gas i over gas j is then expressed by Equation:

$$S_{i/j} = \frac{H_i}{H_j} \quad (3)$$

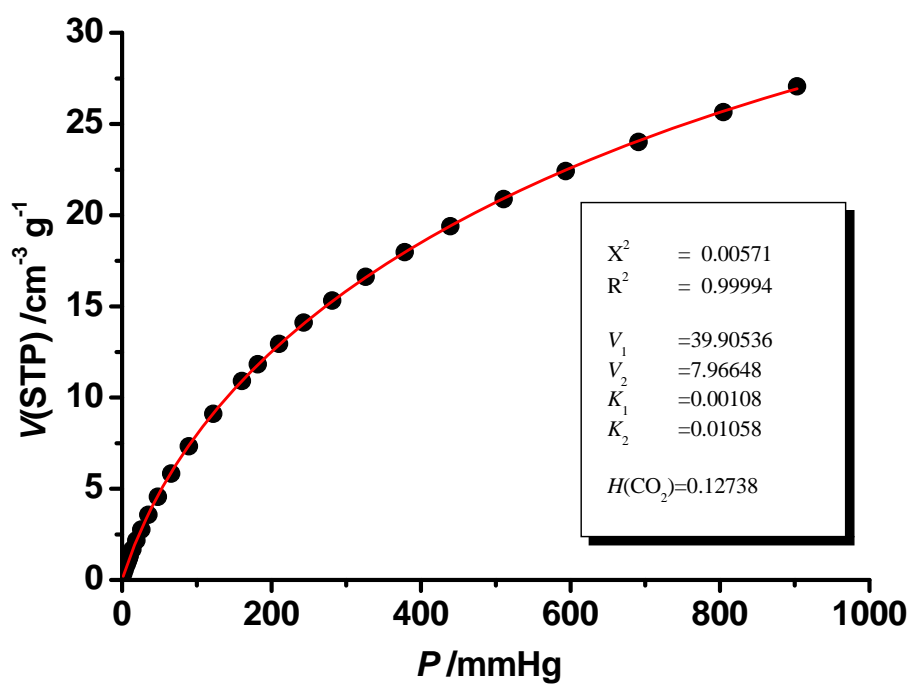


Figure S6. CO_2 isotherm adsorption branch of **1** (filled shape) and fitting based on dual-site Langmuir isotherm model (red line). X^2 and R^2 , fitting error; H , global Herry's law constant, $H(\text{CO}_2) = K_1 \times V_1 + K_2 \times V_2$ ($\text{cm}^3 \text{g}^{-1} \text{mmHg}^{-1}$).

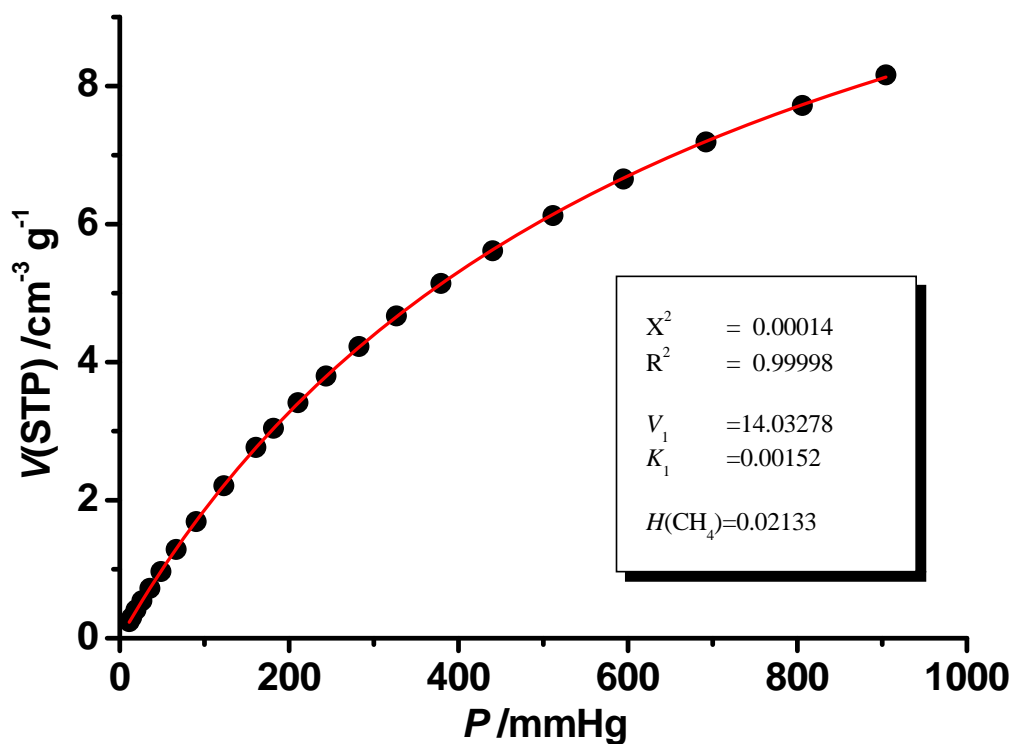


Figure S7. CH_4 isotherm adsorption branch of **1** (filled shape) and fitting based on single Langmuir isotherm model (red line). V_1 , calculated adsorbed volume of CH_4 ; K_1 , calculated affinity constants; X^2 and R^2 , fitting error; H , Herry's law constant, $H(\text{CH}_4)=K_1 \times V_1$ ($\text{cm}^3 \text{g}^{-1} \text{mmHg}^{-1}$).

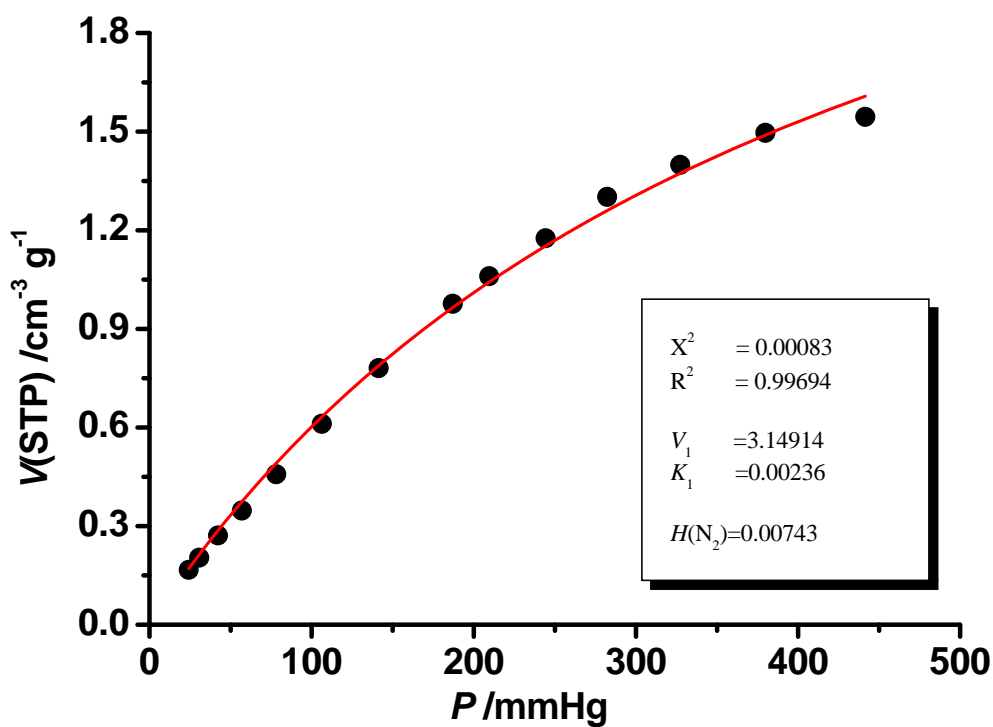


Figure S8. N_2 isotherm adsorption branch of **1** (filled shape) and fitting based on single Langmuir isotherm model (red line). V_1 , calculated adsorbed volume of N_2 ; K_1 , calculated affinity constants; X^2 and R^2 , fitting error; H , Henry's law constant, $H(\text{N}_2) = K_1 \times V_1$ ($\text{cm}^3 \text{g}^{-1} \text{mmHg}^{-1}$).

The Henry's law selectivity can also be calculated based on Toth isotherm model.⁽²⁾

Toth model:

$$M = \frac{M_{\max} \cdot B^{1/n} \cdot P}{(1 + B \cdot P)^{1/n}} \quad (4)$$

M , gas uptake (mmol/g); M_{\max} , maximum gas uptake (mmol/g); B and n , fitting constants.

Henry's law constant H :

$$H = \lim_{P \rightarrow 0} \frac{dN}{dP} = B^{1/n} \cdot M_{\max} \quad (5)$$

Henry's law selectivity (upper limit selectivity), gas component i over j :

$$S_{i/j} = \frac{H_i}{H_j} \quad (6)$$

All fittings and calculations (Figures S11-S13) were performed based on the mean value of each data set.

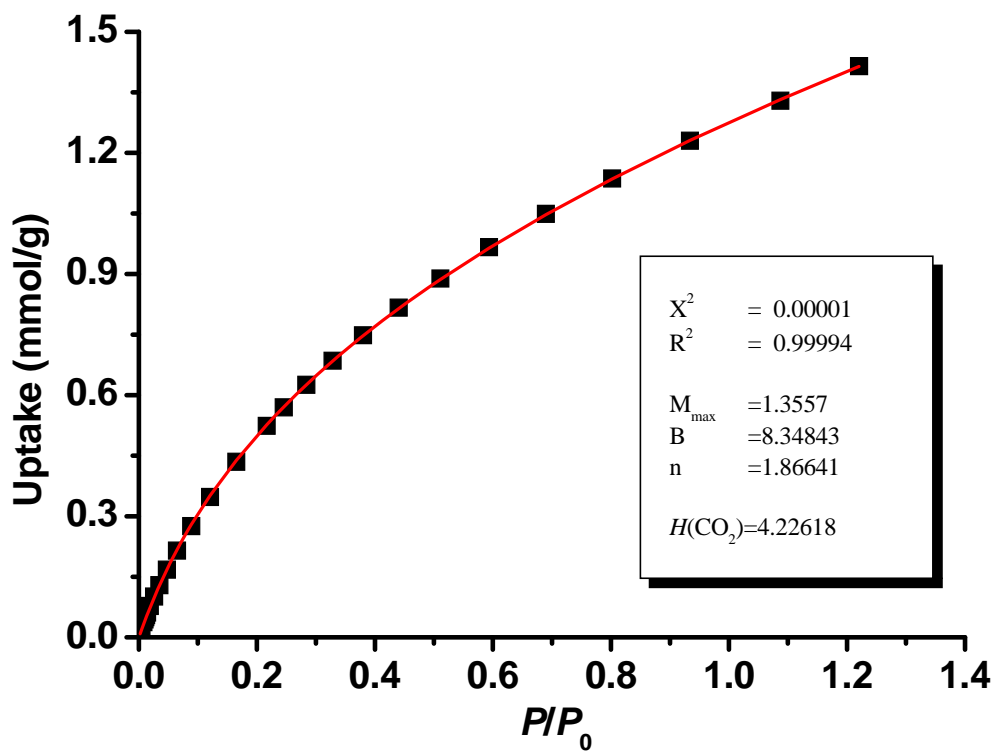


Figure S9. CO_2 isotherm adsorption branch of **1** (filled shape) and fitting based on Toth isotherm model (red line); M_{\max} , maximum uptake; B and n, fitting constants; X^2 and R^2 , fitting error; H , Henry's law constant.

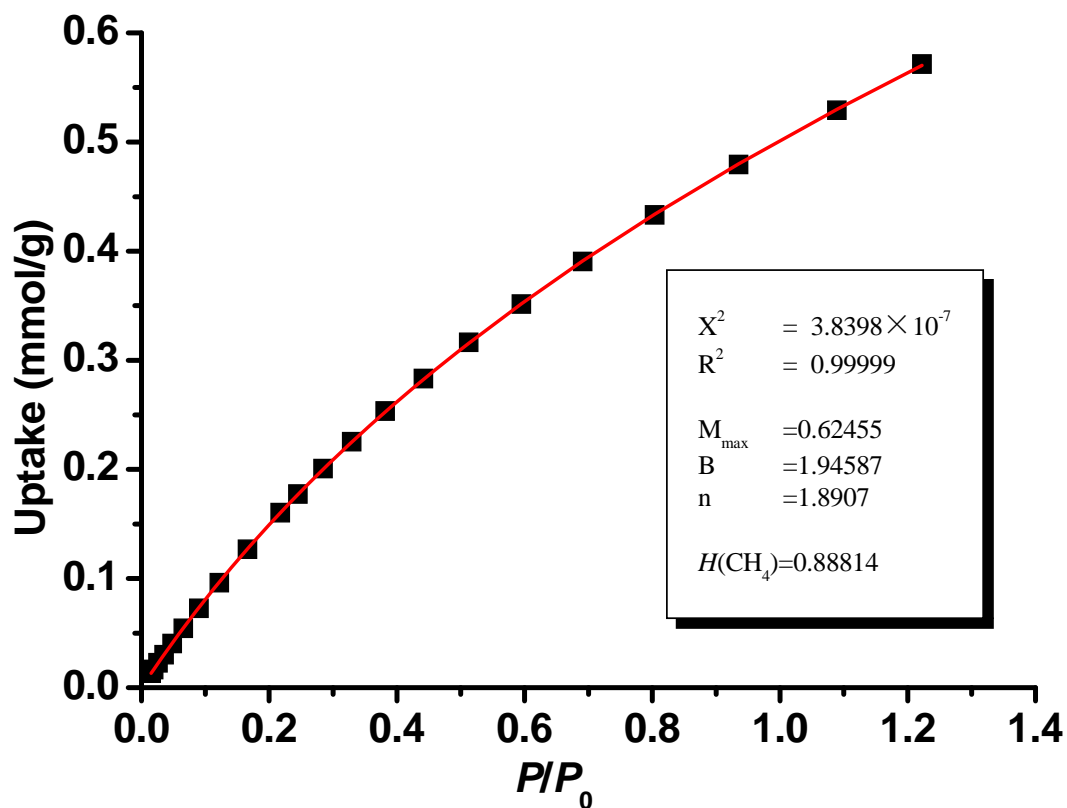


Figure S10. CH_4 isotherm adsorption branch of **1** (filled shape) and fitting based on Toth isotherm model (red line); M_{\max} , maximum uptake; B and n , fitting constants; X^2 and R^2 , fitting error; H , Henry's law constant.

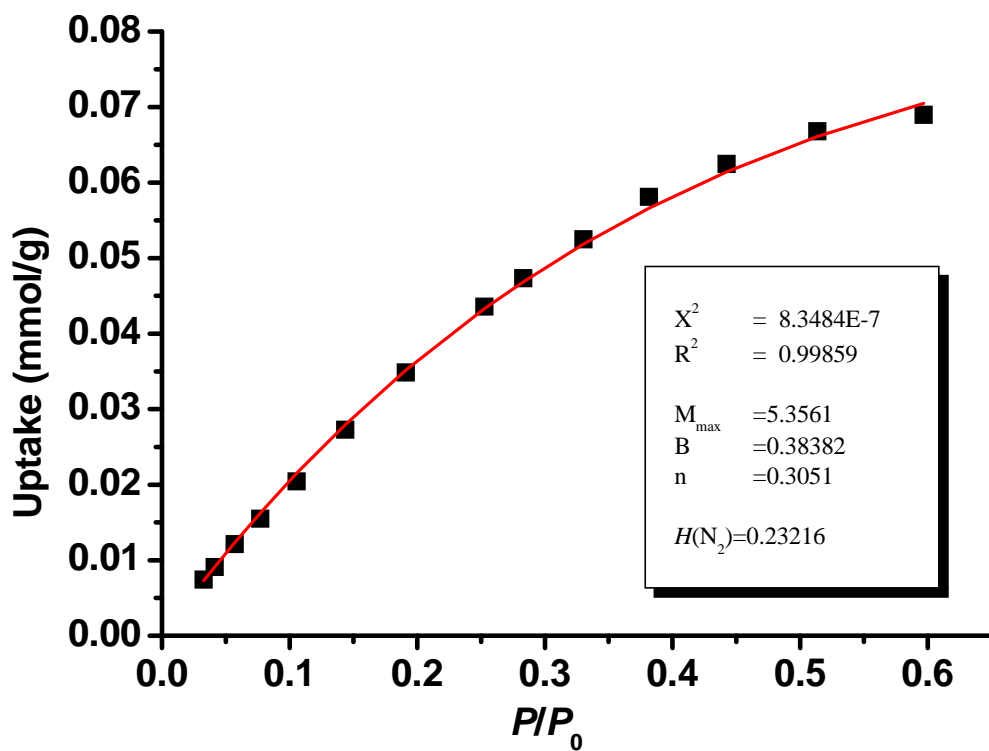


Figure S11. N_2 isotherm adsorption branch of **1** (filled shape) and fitting based on Toth isotherm model (red line); M_{\max} , maximum uptake; B and n, fitting constants; X^2 and R^2 , fitting error; H , Henry's law constant.

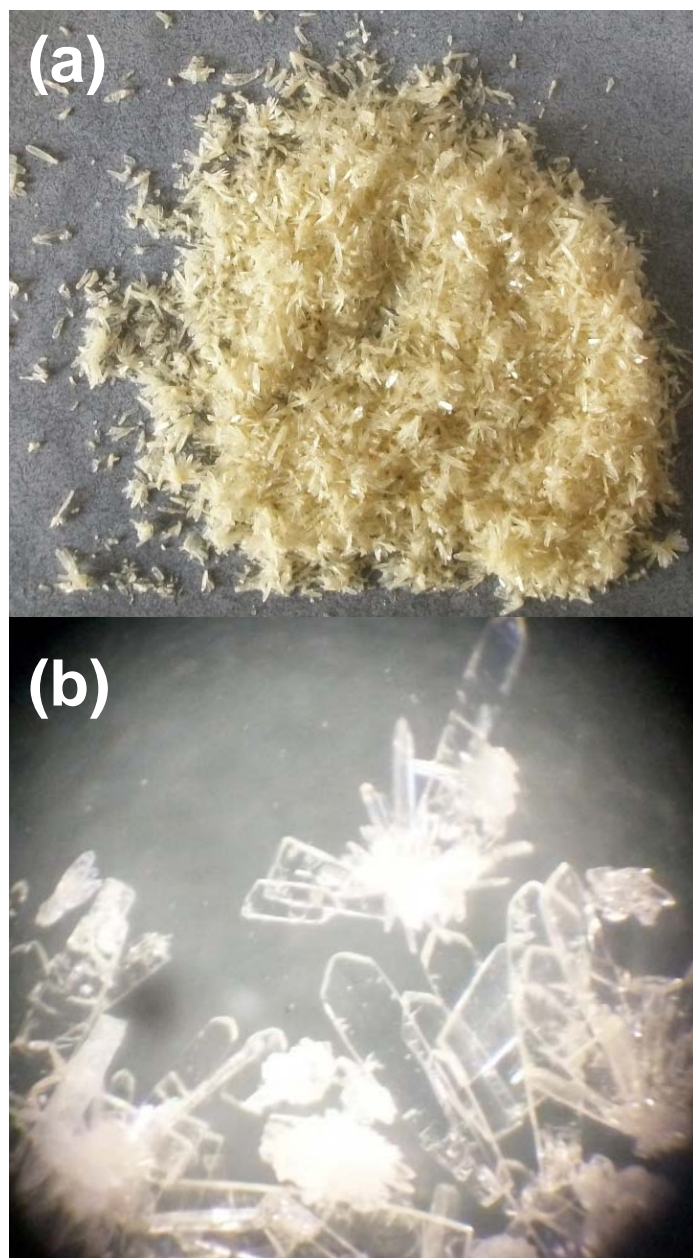


Figure S12. Photograph of raw sample of **1** (a) and image under optical microscope (b).
The average dimension of crystal size is 1.10 mm \times 0.20 mm \times 0.16 mm.

Reference:

- (1) Ortiz G.; Brandes S.; Rousselin Y.; Guillard R. *Chem. Eur. J.* **2011**, *17*, 6689.
- (2) Wang B.; Cote A. P.; Furukawa H.; O’Keeffe M.; Yaghi O. M. *Nature* **2008**, *453*, 207.